

Properties of negative thermal expansion β -eucryptite ceramics prepared by spark plasma sintering

Li-Min Zhao(赵利敏), Yong-Guang Cheng(程永光), Hao-Shan Hao(郝好山), Jiao Wang(王娇), Shao-Hui Liu(刘少辉), Bao-Sen Zhang(张宝森)

Citation: Chin. Phys. B . 2018, 27(9): 096501. **doi:** 10.1088/1674-1056/27/9/096501

Journal homepage: http://cpb.iphy.ac.cn; http://iopscience.iop.org/cpb

What follows is a list of articles you may be interested in

Phase transition and near-zero thermal expansion of $Zr_{0.5}Hf_{0.5}VPO_7$

Jun-Ping Wang(王俊平), Qing-Dong Chen(陈庆东), Sai-Lei Li(李赛磊), Yan-Jun Ji(纪延俊), Wen-Ying Mu(穆文英), Wei-Wei Feng(冯伟伟), Gao-Jie Zeng(曾高杰), You-Wen Liu(刘友文), Er-Jun Liang(梁二军)

Chin. Phys. B . 2018, 27(6): 066501. **doi:** 10.1088/1674-1056/27/6/066501

Negative thermal expansion and photoluminescence in solid solution $(HfSc)_{0.83}W_{2.25}P_{0.83}O_{12\delta}$

Yuan Liang(梁源), Yong-Guang Cheng(程永光), Xiang-Hong Ge(葛向红), Bao-He Yuan(袁保合), Juan Guo(郭娟), Qian Sun(孙强), Er-Jun Liang(梁二军)

Chin. Phys. B . 2017, 26(10): 106501. **doi:** 10.1088/1674-1056/26/10/106501

Anomalous low-temperature heat capacity in antiperovskite compounds

Xin-Ge Guo(郭新格), Jian-Chao Lin(林建超), Peng Tong(童鹏), Shuai Lin(蔺帅), Cheng Yang(杨骋), Wen-Jian Lu(鲁文建), Wen-Hai Song(宋文海), Yu-Ping Sun(孙玉平)

Chin. Phys. B . 2017, 26(2): 026501. **doi:** 10.1088/1674-1056/26/2/026501

Zero and controllable thermal expansion in $HfMgMo_{3-x}W_xO_{12}$

Tao Li(李涛), Xian-Sheng Liu(刘献省), Yong-Guang Cheng(程永光), Xiang-Hong Ge(葛向红), Meng-Di Zhang(张孟迪), Hong Lian(连虹), Ying Zhang(张莹), Er-Jun Liang(梁二军), Yu-Xiao Li(李玉晓)

Chin. Phys. B . 2017, 26(1): 016501. **doi:** 10.1088/1674-1056/26/1/016501

Near-zero thermal expansion of $In_{2(1-x)}(HfMg)_xMo_3O_{12}$ with tailored phase transition

Yong-Guang Cheng(程永光), Yan-Chao Mao(毛彦超), Xain-Sheng Liu(刘献省), Bao-He Yuan(袁保合), Ming-Ju Chao(晁明举), Er-Jun Liang(梁二军)

Chin. Phys. B . 2016, 25(8): 086501. **doi:** 10.1088/1674-1056/25/8/086501

Properties of negative thermal expansion β-eucryptite ceramics prepared by spark plasma sintering*

Li-Min Zhao(赵利敏), Yong-Guang Cheng(程永光), Hao-Shan Hao(郝好山)†, Jiao Wang(王娇), Shao-Hui Liu(刘少辉), and Bao-Sen Zhang(张宝森)

School of Science, Henan Institute of Engineering, Zhengzhou 451191, *China*

(Received 26 March 2018; revised manuscript received 16 June 2018; published online 28 August 2018)

β-eucryptite powders are prepared by the sol–gel method through using tetraethoxysilane lithium nitrate and aluminum isopropoxide as starting materials. β-eucryptite ceramics are prepared by spark plasma sintering. The effects of sintering temperature on the negative thermal expansion properties of the β-eucryptite are investigated by x-ray diffraction (XRD), scanning electron microscopy, and thermal expansion test. The XRD results exhibit no change in the crystal structure of the sample prepared by different sintering processes. The negative thermal expansion properties increase with the increase of the sintering temperature. The coefficient of thermal expansion of β-eucryptite ceramics sintered at 1100 °C is calculated to be -4.93×10^{-6} °C^{-1}. Crystallization behaviors of the ceramics may play an important role in the increase of negative thermal expansion of β-eucryptite. High sintering temperature could improve the crystallization behaviors of the ceramics and reduce the residue glass phase, which can improve the negative thermal expansion properties of β-eucryptite ceramics.

Keywords: β-eucryptite, thermal expansion, structure, spark plasma sintering

PACS: 65.40.De, 67.80.de, 81.20.Ev **DOI:** 10.1088/1674-1056/27/9/096501

1. Introduction

In recent years, near-zero or controllable expansion materials have attracted a great deal of attention due to their potential applications in precision devices and instrument equipments in high-tech systems, and microelectronic or optical precision applications.[1–5] For example, negative thermal expansion materials reinforced Cu matrix composites have wide applications in thermal management materials, which are gradually becoming a hot issue.[6–8] These near-zero or controllable expansion materials are mainly obtained by designing their composite materials with positive and negative thermal expansions. Thus far, only a few types of negative thermal expansion materials have been prepared, including AM_2O_8 (A = Zr, Hf; M = W or Mo), $A_2M_3O_{12}$ (A = trivalent transition metal or rare earth), cyanides $M(CN)_2$ (M = Zn, Cd) and $Ag_3[Co(CN)_6]$, fluorides ScF_3, phosphides $NaZr_2P_3O_{12}$, vanadates ZrV_2O_7, β-eucryptite, etc. Among the negative thermal expansion materials, β-eucryptite has attracted a great deal of attention in recent years due to its stable nature in structure at room temperature and negative thermal expansion in a wide temperature range.[9–11]

Conventionally, solid state reaction is a common method to prepare β-eucryptite powers. The synthesis process is simple, but there will be some impurities in the sample. The sol–gel method has been considered to be a promising method of preparing β-eucryptite powers with the advantages of high purity, lower sintering temperature, and high degree of homogeneity. Naskar and Chatterjee synthesized β-eucryptite powders through the sol–gel technique and investigated the substantial crystallization of β-eucryptite powders.[12] Some different sintering methods, including conventional sintering, hot pressing sintering, glass-forming technique, and spark plasma sintering, have been used to manufacture β-eucryptite ceramics. The traditional method of preparing β-eucryptite ceramics is the glass-forming technique.[13,14] This method includes preparation of molten materials, shaping, and recrystallization. Effects of the nucleating agent and crystallization behavior on the negative thermal expansion properties of the β-eucryptite were investigated. However, the β-eucryptite ceramics manufactured by this method are sometimes inhomogeneous, which fail to meet the rigorous requirements of applications. Conventional sintering is another method of preparing the β-eucryptite ceramics. This method is simple, versatile, and convenient. However, β-eucryptite ceramics prepared by this method usually show low mechanical strength because the expansion anisotropy causes micro cracking at the high sintering temperature. It is difficult to obtain dense β-eucryptite ceramics at low temperatures.[15–19] The β-eucryptite ceramics fabricated by spark plasma sintering are proposed as a solution to these problems. The spark plasma sintering can lead to high relative densities and homogeneous distribution. Much effort

*Project supported by the Programs for Tackling Key Problems in Science and Technology, Henan Province, China (Grant Nos. 172102210103, 182102310895, 182102210031, and 182102311079), the Doctoral Program of Henan Institute of Engineering, China (Grant Nos. D2016015 and D2016016), and the National-level College Students Innovative Entrepreneurial Training Plan Program, China (Grant No. 201611517041).

†Corresponding author. E-mail: hshhao@126.com

© 2018 Chinese Physical Society and IOP Publishing Ltd

has been made to prepare the β-eucryptite ceramics with excellent negative thermal expansion performance via the glass-forming technique and powders prepared by solid state reaction followed by conventional sintering. Little attention has been paid to the β-eucryptite ceramics via powders prepared by the sol–gel method followed by spark plasma sintering.

In this paper, β-eucryptite ceramics are prepared by the sol–gel method and followed by spark plasma sintering. The microstructure and thermal expansion behavior of β-eucryptite ceramics sintered at different sintering temperatures are investigated by x-ray diffraction (XRD), scanning electron microscopy, and dilatometer. The physical mechanism for the improvement of thermal expansion behavior is also discussed.

2. Experimental section

β-eucryptite ceramics powders were synthesized via a sol–gel method by using tetraethoxysilane (TEOS), lithium nitrates ($LiNO_3$), and aluminum isopropoxide ($C_9H_{21}AlO_3$) as starting materials. The TEOS was first added into an equal volume of ethanol and half the volume of distilled water, to obtain the TEOS solution. A few drops of HCl were added to adjust the pH of the solution. An aqueous nitrate solution was prepared by mixing appropriate amounts of $C_9H_{21}AlO_3$ and $LiNO_3$, and then added to the stoichiometric quantity of the TEOS solution. The mixture was stirred at room temperature to obtain a gel, which was then dried at about 70 °C to obtain amorphous powders. These powders were then calcined in air at 600 °C for 2 h.

The resulting powders were loaded into a 10 mm-diameter graphite die, then a pressure of about 50 MPa was applied. Then the temperature was raised separately to different sintering temperatures (800 °C, 900 °C, 1000 °C, 1100 °C) at a rate of 100 °C/min and was kept at the temperature for 5 min followed by slow cooling.

3. Characterization

The crystal structures of the samples sintered at different temperatures were investigated by XRD (D8 Advanced, Bruker, Germany) with Cu $K\alpha$ radiation, scanning from 10° to 80°. Temperature-dependent intrinsic (lattice) measurements were carried out in a temperature range from room temperature (RT) to 800 °C using high temperature x-ray diffraction (HTXRD) (D8 advance Bruker, Germany, equipped with a furnace). The XRD spectra were analyzed by using Topas software (Bruker). The microstructures of β-eucryptite sintered samples were investigated by scanning electron microscopy (XL30-FEG, Philips, Netherlands). Cross-sections of the specimens were etched with approximately 5 vol.% HF solution for 60 s to remove the glass phases for observing the crystal distribution clearly. The negative thermal expansion properties from RT to 800 °C were measured in air using a dilatometer (LINSEIS DIL L75, Germany) at a heating rate of 5 °C/min in ambient atmosphere.

4. Results and discussion

The XRD patterns of β-eucryptite ceramics prepared by spark plasma sintering at different temperatures are shown in Fig. 1. As can be seen, the peaks correspond to β-eucryptite (PDF#12-0709) and there is no visible signal of secondary phases in the samples. The intensities of the major diffraction peaks of β-eucryptite crystals increase initially with sintering temperature increasing, which indicates that the relative content of β-eucryptite crystal increases with the increase of the sintering temperature.

The calculated amount of the β-eucryptite phase in the sintered body is determined by the integrated intensity of the strongest peak of the β-eucryptite phase as a measure. The degree of crystalline is evaluated from the following formula:

$$X_c = \frac{\sum_i I_{ci}}{\sum_i I_{ci} + KI_a},$$

where X_c is the crystalline degree, I_a is the integrated intensity of the non crystalline phase, I_{ci} is the integrated intensity of the crystalline phase, and K ($K = 0.963$) is a constant relating to the measurement condition. It indicates that the relative crystalline degree of β-eucryptite increases considerably from 64% to 88.2% as the sintering temperature increases from 800 °C to 1000 °C and the relative crystalline degree increases slowly from 88.2% to 89.2% as the temperature increases from 1000 °C to 1100 °C, implying the near completion of the crystalline process.

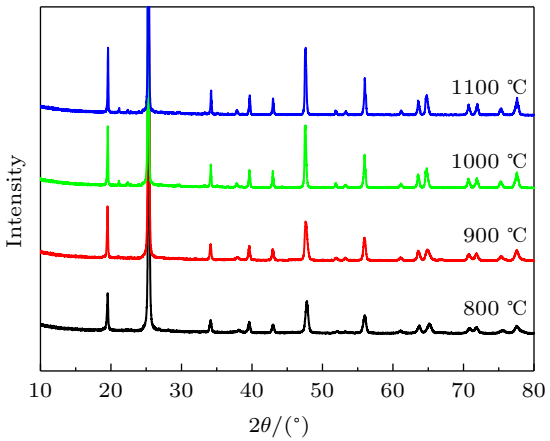


Fig. 1. (color online) XRD patterns of the surfaces of β-eucryptite ceramics sintered at different temperatures.

The SEM images of cross sections of β-eucryptite ceramics sintered at 800 °C and the etched β-eucryptite ceramics sintered at different temperatures are given in Fig. 2. Figure 2(a) shows an SEM image for the cross section of β-eucryptite ceramics sintered at 800 °C. It is difficult to observe the grain distribution because the β-eucryptite ceramics have

many glass phases. To remove the glass phases, the cross-section of the sample is etched with HF solution. The porosity in the β-eucryptite ceramic sample is observed after the glass phase has been etched by the HF solution. The porosity number in the β-eucryptite ceramic sample decreases as the sintering temperature increases. Compared with β-eucryptite ceramics sintered at 800 °C, 900 °C, and 1000 °C, β-eucryptite ceramic sintered at 1100 °C shows small porosity. This is due to the reduced glass phase with the increase of the sintering temperature. Furthermore, the average grain size of the β-eucryptite ceramic sample increases as the sintering temperature increases. When β-eucryptite ceramic is sintered at 800 °C, the average size of the grains is about 400 nm and the grains distribute uniformly as shown in Fig. 2(b). When the sintering temperature is higher than 900 °C, the grains begin to grow up and the average size of the grains of the β-eucryptite ceramic sintered at 1100 °C is about 1 μm.

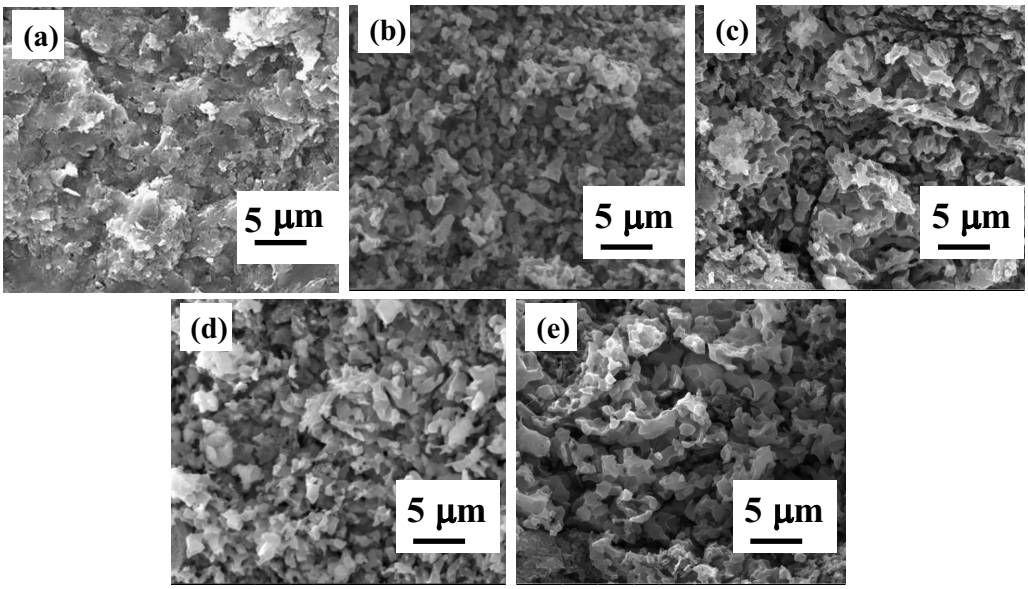


Fig. 2. (color online) SEM images of cross sections of (a) β-eucryptite ceramics sintered at 800 °C and the etched β-eucryptite ceramics sintered for 5 min at different temperatures: (b) 800 °C, (c) 900 °C, (d) 1000 °C, and (e) 1100 °C.

Figure 3 shows the relative length changes of β-eucryptite ceramics measured from RT to 800 °C for the samples sintered at different temperatures. It can be seen that the relative length change of the β-eucryptite ceramic sintered at 800 °C decreases with the increase of the measuring temperature when the temperature is lower than 400 °C, and then increases when the temperature is higher than 400 °C. The origin of the negative thermal expansion of β-eucryptite on the crystal structure is closely related to the change of structure with temperature.[20,21] Schematic diagrams of β-eucryptite structure plan and profile are shown in Fig. 4. The structures of β-eucryptite involve tetrahedron clearance and octahedral clearance. The Li atoms can occupy sites which are surrounded by tetrahedron clearance or octahedral clearance. The occupation possibility of these clearances depends on the temperature. The Li atoms occupy tetrahedron clearance at about room temperature. The octahedral clearance occupation possibility by Li atoms increases with the temperature increasing. Some octahedral clearances of β-eucryptite are occupied by Li atoms at higher temperatures. When octahedral clearance is occupied by an Li atom, the $(Si,Al)O_2$ framework around this site is influenced by the occupying atom. The framework in the immediate neighborhood of the Li atoms expands parallel to the a axis and contracts parallel to the c axis. The occupied octahedral clearance number increases and then the a axis increases and the c axis decreases with the temperature increasing. The positive thermal expansion of the residue glass phase can counteract the negative thermal expansion of the β-eucryptite phase. The β-eucryptite ceramic sintered 800 °C shows negative thermal expansion from RT to 400 °C. The sudden positive thermal expansion from 400 °C to 800 °C is possible due to a glass phase with obvious positive volume expansion. The β-eucryptite ceramics sintered at 900 °C, 1000 °C, and 1100 °C exhibit continuous negative thermal expansions in a large temperature range from RT to 800 °C because of the decrease of the glass phase. Moreover, we can also find that the negative thermal expansion property increases with sintering temperature increasing. Compared with other samples, β-eucryptite ceramic sintered at 1100 °C shows a better negative thermal expansion property in the whole measuring temperature range.

The coefficients of thermal expansion of β-eucryptite ceramics from RT to 800 °C are calculated from the formula

$\alpha = (1/L_0) \cdot (\mathrm{d}L/\mathrm{d}T)$, and the results are shown in Fig. 5. It can be observed that the coefficient of thermal expansion of β-eucryptite ceramics increases with sintering temperature increasing, and it is -4.93×10^{-6} °C^{-1} for the sample sintered at 1100 °C. The reason can be attributed to the crystallization behaviors. High sintering temperature can improve the crystallization behaviors of ceramics and reduce the residue glass phase, which is favorable to enhancing the negative thermal expansion of β-eucryptite ceramic.[22] The XRD analysis and SEM results clarify this point and it is in agreement with the HTXRD analyses.

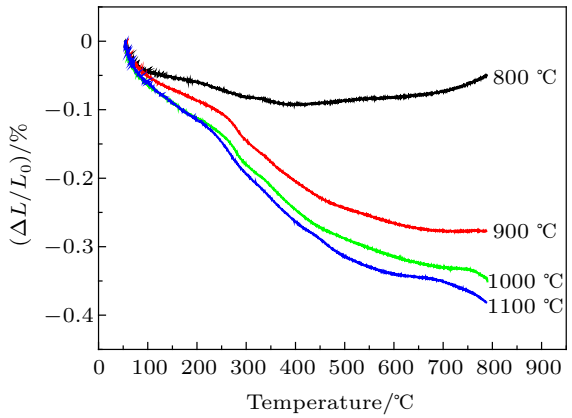


Fig. 3. (color online) Relative length changes of β-eucryptite ceramics with temperature, measured from RT to 800 °C for the samples sintered at different temperatures.

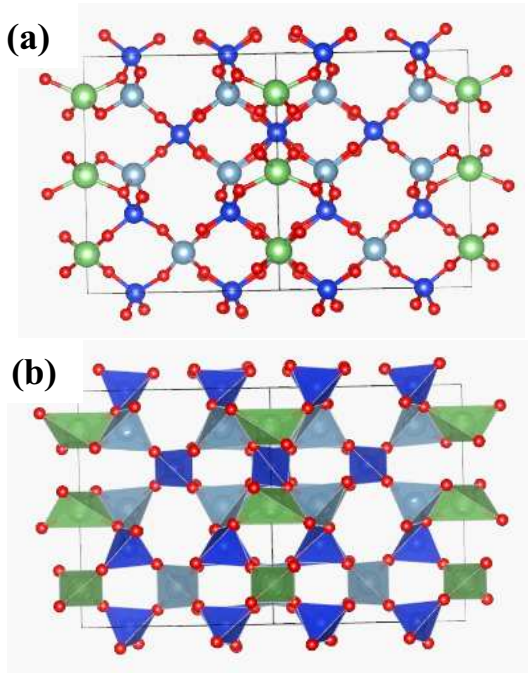


Fig. 4. (color online) Schematic diagrams of β-eucryptite structure: (a) plan, (b) profile.

To confirm the intrinsic negative thermal expansion property, we measure the temperature-dependent XRD patterns of β-eucryptite powders sintered at 1100 °C and the results are shown in Fig. 6(a). The XRD results exhibit no change of

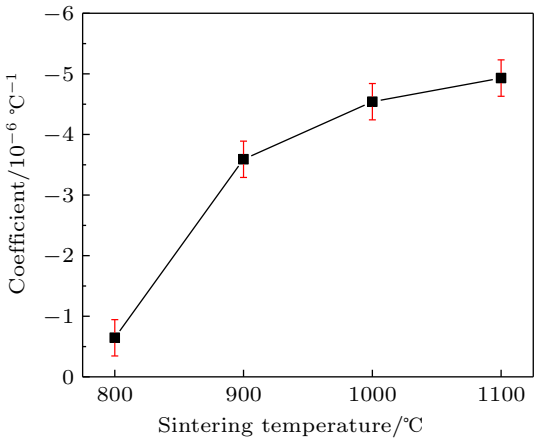


Fig. 5. (color online) Coefficient of thermal expansion calculated from RT to 800 °C for the samples sintered at different temperatures.

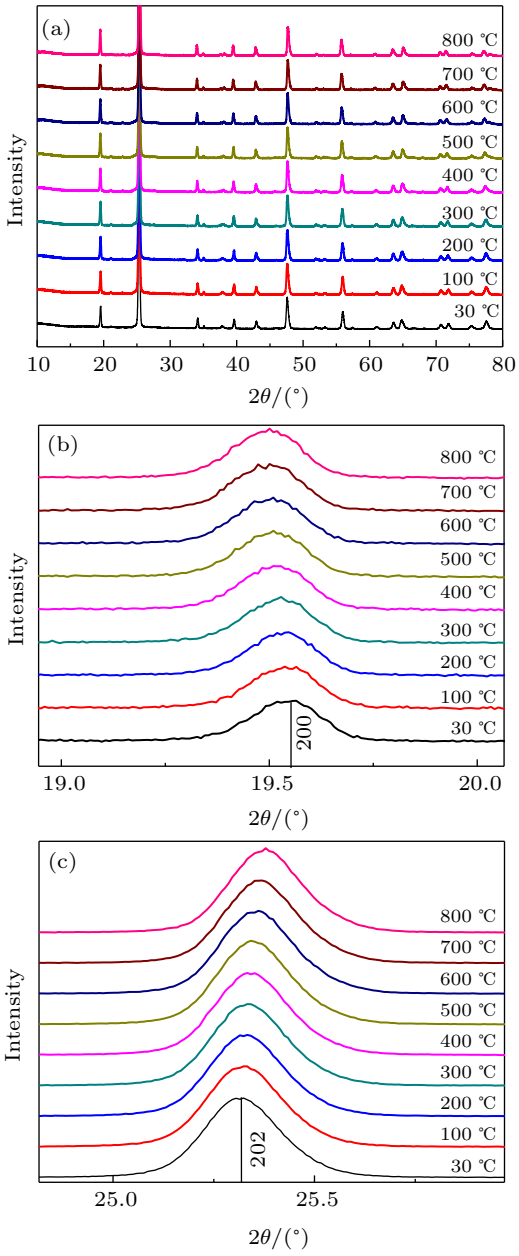


Fig. 6. (color online) (a) Temperature-dependent XRD patterns from RT to 800 °C for β-eucryptite powders sintered at 1100 °C. Temperature dependence of (b) (200) and (c) (202) characteristic peaks.

the crystal phase, but the angles of the diffraction peaks shift with the increase of the measuring temperature. Figures 6(b) and 6(c) show the temperature dependence of (200) and (202) characteristic peaks. As seen in Fig. 6(b), the (200) diffraction peak shifts toward a low angle with the increase of the measuring temperature, which indicates that the lattice constant of the a-axis is enhanced with the increase of the measuring temperature; while the (202) characteristic peak shifts toward a high angle with the increase of the measuring temperature, which indicates that the lattice constant of the c-axis decreases with the increase of the measuring temperature.

Figure 7(a) shows the thermal evolution of the lattice parameters a and c of β-eucryptite powder calculated by HTXRD in a temperature between RT and 800 °C. The a-axis monotonically expands from 10.477 Å to 10.505 Å and the c-axis monotonically decreases from 11.113 Å to 11.011 Å when the measuring temperature increases from RT to 800 °C. The calculated volumes at each temperature are shown in Fig. 7(b). The volume decreases from 1057.5 $Å^3$ to 1052.5 $Å^3$ with the increase of temperature. It is the dramatic decrease of the c-axis in the β-eucryptite that results in the negative thermal expansion in volume. These results confirm the negative thermal expansion property measured by dilatometers. The schematic of thermal expansion in β-eucryptite ceramic is shown in Fig. 8. The two-dimensional expansion occurs in β-eucryptite with the increase of temperature. Compared with the a axis stretching, the c axis is forcibly pulled closer together, which leads to a significant thermal contraction in the c-axis direction.[20] The β-eucryptite structure is a stuffed derivative of the high-quartz structure where half of the Si^{4+} ions are replaced by Al^{3+} ions and their charges are balanced by Li^+ ions. The thermal expansion behavior of β-eucryptite is closely related to its structure.[23]

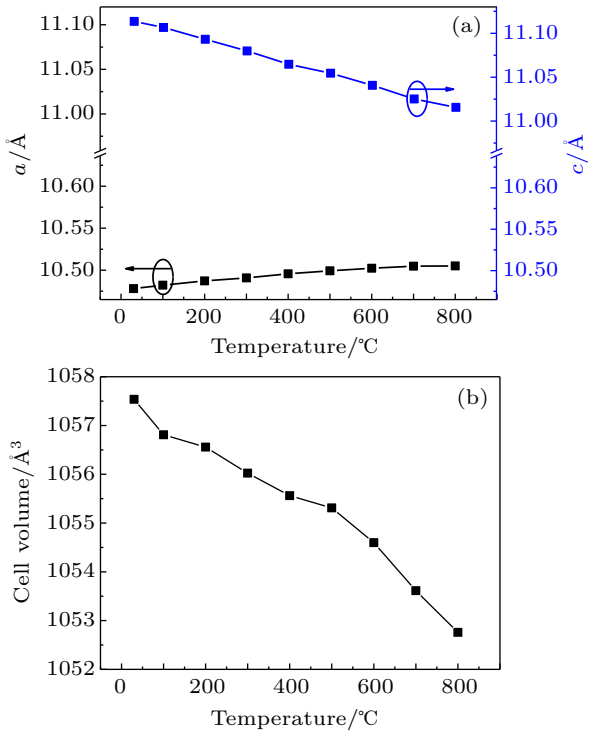


Fig. 7. (color online) Changes of (a) lattice constants and (b) volume with temperature.

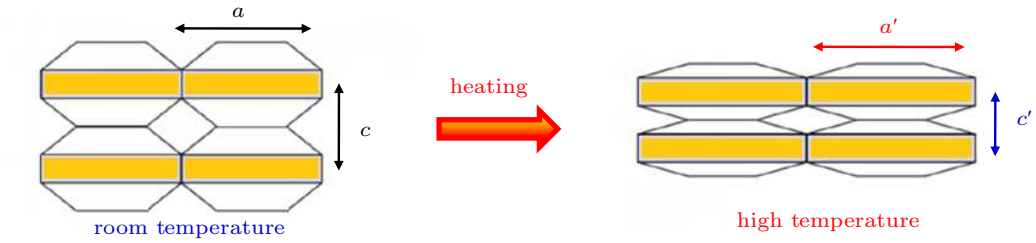


Fig. 8. (color online) Schematic of thermal expansion in β-eucryptite ceramic.

5. Conclusion

The β-eucryptite powders are prepared by the sol–gel method, and the ceramics are prepared by spark plasma sintering. The effects of sintering temperature on crystal structure, microstructure, and negative thermal expansion properties of β-eucryptite ceramics are investigated. The results show that the negative thermal expansion property increases with sintering temperature increasing. The coefficient of thermal expansion of β-eucryptite ceramic sintered at 1100 °C is -4.93×10^{-6} °C^{-1} from RT to 800 °C. The XRD and SEM verify that the crystallization behaviors of ceramics increase with sintering temperature increasing, which improves the negative thermal expansion property of β-eucryptite ceramic. This study provides an effective way to prepare the β-eucryptite ceramics with relatively high negative thermal expansion performance.

References

[1] Lichtenstein A I, Jones R O, Xu H and Heaney P J 1998 *Phys. Rev. B* **58** 6219
[2] Li T, Liu X S, Cheng Y G, Ge X H, Zhang M D, Lian H, Zhang Y, Liang E J and Li Y X 2017 *Chin. Phys. B* **26** 016501
[3] Pelletant A, Reveron H, Chêvalier J, Fantozzi G, Blanchard L, Guinot F and Falzon F 2012 *Mater. Lett.* **66** 68
[4] Fei W D and Wang L D 2004 *Mater. Chem. Phys.* **85** 450
[5] Fedorova A, Hourlier D and Scheffler M 2017 *Ceram. Int.* **43** 4483
[6] Sheng J, Wang L, Li S, Yin B, Liu X and Fei W D 2016 *Sci. Rep.* **6** 27118
[7] Xue Z W, Wang L D, Liu Z and Fei W D 2010 *Scr. Mater.* **62** 867

[8] Sheng J, Wang L D, Li D, Cao W P, Feng Y, Wang M, Yang Z Y, Zhao Y and Fei W D 2017 *Mater. & Design* **132** 442
[9] Chen Y, Manna S, Narayanan B, Wang Z, Reimanis I E and Ciobanu C V 2016 *Scr. Mater.* **122** 64
[10] Cooper R C, Bruno G, Wheeler M R, Pandey A, Watkins T R and Shyam A 2017 *Acta Mater.* **135** 361
[11] Benavente R, Salvador M D, Martínez-Amesti A, Fernández A and Borrell A 2016 *Mater. Sci. Eng.: A* **651** 668
[12] Naskar M K and Chatterjee M 2005 *Mater. Lett.* **59** 998
[13] Stanislavchuk T N, Middlemiss D S, Syzdek J S, Janssen Y, Basistyy R, Sirenko A A, Khalifah P G, Grey C P and Kostecki R 2017 *J. Appl. Phys.* **122** 045107
[14] Choi D S 2016 *Appl. Sci. Convergence Technol.* **25** 116
[15] Marcial J, Ahmadzadeh M and McCloy J S 2017 *MRS Adv.* **2** 549
[16] Cheng Y, Liang Y, Ge X, Liu X, Yuan B, Guo J, Chao M J and Liang E J 2016 *RSC Adv.* **6** 53657
[17] Gokhe U B, Koparkar K A and Omanwar S K 2016 *J. Alloys Compd.* **689** 992
[18] Jeong B J, Joung M R, Kweon S H, Kim J S, Nahm S, Choi J W and Hwang S J 2012 *J. Am. Ceram. Soc.* **95** 1811
[19] Ramalingam S and Reimanis I E 2012 *J. Am. Ceram. Soc.* **95** 2939
[20] Takenaka K 2012 *Sci. Technol. Advanced Mater.* **13** 013001
[21] Schulz H 1974 *J. Am. Ceram. Soc.* **57** 313
[22] Xia L, Wen G W, Song L and Wang X Y 2010 *Mater. Chem. Phys.* **119** 495
[23] Schuld S, Diekmann M, Schäfer M and Weitzel K M 2016 *J. Appl. Phys.* **120** 185102